

# Humanoid Movement

From Human Motion to Humanoid Control - Ecole Centrale Nantes

Rudra Patel

Student ID: 1904910

Rudra.Patel@eleves.ec-nantes.fr

Steven Palma Morera

Student ID: 200443K

steven.palma-morera@eleves.ec-nantes.fr

**Abstract**—This report contains discussions on the measurement of the Human Motion to Humanoid Control Lab [1]. First, the BSP parameters of a subject are calculated to obtain the modified Hanavan model. Then, several motions are measured and by using the Newton Euler recursive algorithm, the ground reaction efforts are computed, visualized and compared against the measured ones using MATLAB.

**Index Terms**—Human Motion, Motion Capture, Newton-Euler, MATLAB

## I. INTRODUCTION

Several body motions performed by a subject are registered by measuring the position and orientation at each time-step of 20 different markers placed along his body. These measurements are obtained using the Motion Capture software and are then used as inputs for a Newton-Euler backward and forward algorithm with the objective of estimating the reaction efforts applied on the ground. Moreover, the efforts applied on the ground by the subject while performing the motion are measured by a force plate sensor. This data-set is then compared against the results obtained from the Newton-Euler algorithm developed. In the following sections the reader can find the steps followed to obtain the data-sets and to design the programmatic functions explained very briefly, discussing mainly the important assumptions or design decisions taken. The main focus of the report is in the analysis of the results obtained and their relationship with the Human Motion to Humanoid Control topics. All the images shown in this document are of own elaboration and were obtained by testing the lab using Windows 10, MATLAB 2020 on December 15th, 2020. The full repository of the lab can be found [here](#).

## II. GETTING THE MEASUREMENTS

Three main data-sets have to be obtained: The BSP Parameters of the subject, the Motion Capture markers and the Ground Plate reaction efforts for each motion. The BSP parameters are used for estimating the physical dimensions of the body of the subject. For a correct estimation of the BSP parameters, multiple measurements of his body parts have to be performed repetitively. Unfortunately due to the COVID pandemic, this kind of experimentation was not possible. So, we were given 5 similar sets of the 41 parameters of the same subject required for modified Hanavan predictive model. Similarly for the Motion Capture and Force Plate data-set, the “.drf” and “.csv” files for several different motions were already given due the

COVID limited situation. It is important to notice that the Motion Capture and the Ground Plate data-sets don’t have the same frequency of measurement, the first works at 60 Hz frequency while the last works at 1000 Hz. The following motions were fully recorded and provided beforehand:

- 1) Waving Right arm at slow, medium and fast velocities.
- 2) Kicking Right foot motions at slow, medium and fast velocities.
- 3) Vertical Jump with and without counter movement for short jump, medium jump, a jump as high as possible in extension and other while bringing feet as high as possible.
- 4) Other motions were provided and they can be studied from the program developed; however, they are omitted in this report for sake of brevity.

## III. SIMULATION DESIGN USING MATLAB

### A. BSP Parameters Estimation

The “BSPparameters” function takes as an input the average of the 5 data-sets given for the 41 parameters of the subject. Using these body parts measurements, it categorizes each part as a Semi-Ellipsoid or as a Elliptical Solid geometrical shape, following the Hanavan predictive model. An assumption that each part of the body has a constant density equal to the average density of human body is done, this means that it is assumed that each part has a density equal to  $1000 \text{ kg/m}^3$ . Given then the density and the size of the geometrical shapes, the center of mass, the inertia matrix and the mass of each part of the body is computed, including also the total mass of the subject estimated using this approach.

### B. Reading files

The functions “readDRF” and “readForce” read the relevant information from each given data-set coming from the Motion Capture and force plate sensor. For the Motion Capture data-set, this information includes the timestamp of each measurement and the value of the position and orientation of each marker. These values are then converted to meters and radians respectively. From the force plate data-set, the six components of the effort applied on the ground are extracted ( $[f_x, f_y, f_z, m_x, m_y, m_z]$ ) and are then filtered in two ways. The first filter is to re-sample their frequency to 60 Hz, the same as the Motion Capture sensor, and the second one is to smooth the signal and remove out-liners.

### C. Newton Euler and Energies Algorithm

Making a strong assumption that each part of the subject's body behaves as a rigid body, then the Newton Euler Algorithm can be used to, from the velocities, accelerations and mass of each part of the body, compute the ground reaction efforts applied by the subject for each motion performed. This algorithm is divided in two main parts: the forward and the backward.

1) *Forward Newton Euler*: The forward Newton Euler equations for the efforts of a tree like robot architecture is given in equation 1 and 2.

$$\sum F_i = m_i \ddot{v}_i + \dot{\omega}_i \times m_i S_i + \omega_i \times (\omega_i \times m_i S_i) \quad (1)$$

$$\sum M_i = I_{O_i} \dot{\omega}_i + m_i S_i \times v_i + \omega_i \times (I_{O_i} \omega_i) \quad (2)$$

- i      A body part. i=1,2...number of bodies  
 $m_i S_i$       Distance from the origin of frame i to the center of mass of body i, times the mass of body  
 $I_{O_i}$       Inertia matrix of body i  
 $v_i, \omega_i$       Linear and angular velocity of the frame origin i  
 $\dot{v}_i, \dot{\omega}_i$       Linear and angular acceleration of the frame origin i  
 $F, M$       Force and Moment of body i

The function "NE\_forward" computes the right hand side of the equations shown above for each body part, or from now on called a link. The origin of each link frame is considered to be located where the motion capture marker was placed. Since the position and orientation of each marker is known for each time-step, then the velocity and acceleration of each link's origin frame can be computed. And since from the BSP Parameters, the mass, the inertia matrix and the center of mass of each link is known, then all the right hand side of the equations can be solved individually for each body link. In the Fig.1, the location of each marker, and therefore the location of the origin of each body link, from the Motion Capture in the subject's body is shown.

It is important to notice that the velocity of each link frame is obtained by taking the central difference of its position at each time-step. Similarly for the acceleration, the central difference of the resulted velocity is computed. Following this method, the resulted values tend to be noisy and with peaks. This is why two filters are applied to the velocities and accelerations computed, one two remove the out-liners and one to smooth the signals.

2) *Backward Newton Euler*: The backward Newton Euler equations for the efforts of a tree like robot architecture is given in equation 3 and 4.

$$F_{next} + F_w - F_{past} = \sum F_i \quad (3)$$

$$M_{next} + M_{weight} + M_{F_{next}} - M_{past} = \sum M_i \quad (4)$$

- $F_w$       The weight of the link i  
 $F_{past}$       The force applied to the link i by the previous link  
 $F_{next}$       The force that the link 1 apply to the next link

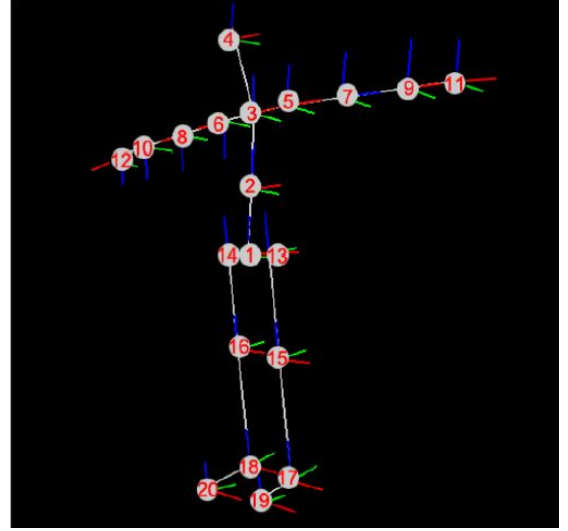


Fig. 1. Location of the markers in the subject's body, also treated as the origin of each link.

- $M_w$       Moment produced by the weight of body i with respect to the frame i origin  
 $M_{F_{next}}$       Moment produced by the force applied to the next body with respect to the frame i origin  
 $M_{past}$       Moment applied to the link i by the previous link  
 $M_{next}$       Moment that the link i apply to the next link

The function "NE\_forward" computes the left hand side of the equations shown above recursively for each sub tree architecture formed by the location of the markers on the subject's body. The following sub trees are considered:

- Right hand= Starting from the frame 12, considered as an end effector of the tree structure and  $F_{past} = 0$ , to the frame 6.
- Left hand= Same as the right hand tree but starting from the frame 11 and finishing in frame 5.
- Head= A simple tree composed only by one link (the head) starting from frame 4 to frame 3.
- Trunk= The forces and moments applied in frame 6 and 5 are translated to frame 3 and then a tree structure starting from frame 3 to frame 1.
- Legs= Starting from 14 and 13 for the right and left leg, respectively and finishing in frame 20 and 19.

The Newton Euler algorithm then is solved for each sub tree, since for each body the left hand side and right hand side of the equations are known or recursively computed. Moreover, two important assumptions were taken. First, it is assumed that the efforts in the frame 1 of Fig.1 are equally distributed in frame 14 and frame 13. Second, the final ground reactions computed by the algorithm are the sum of the resultant efforts of frame 19 and frame 20.

3) *Energies*: Since the velocity and acceleration of each link is known, as well as the mass, its inertia matrix and its center of mass, the potential and kinetic energy of the links can be computed. The functions "energyComputation" and

“energyAllBodies” compute these energies at each time-step following equation 5 and equation 6, assuming  $g = 9.81m/s^2$ .

$$K = \frac{1}{2}(m_i v_i m'_i + w_i I_{O_i} w'_i + 2m S'_i (v'_i \times w)) \quad (5)$$

$$U = -m_i g' r_{O S_i} \quad (6)$$

#### D. Pendulums

In this section we explore the NE equations on single and double inverted pendulums. We first calculate the linear & angular velocities and accelerations for different positions. After defining the position and center of mass we simply calculate the LHS of NE equations. And then using a simple “for loop” we balance the RHS and LHS of the NE equations. what we basically do is extend this formalism to the human body which is shown in the Figure2. We consider a torque controller (motor on the ankle) which is grounded and the mass of the body is located at the mass point of the pendulum.

$$F_{current} = F_{LHS} - (m * g) - F_{next} \quad (7)$$

$$M_{current} = M_{LHS} - (mS \times m * g) - M_{next} \quad (8)$$

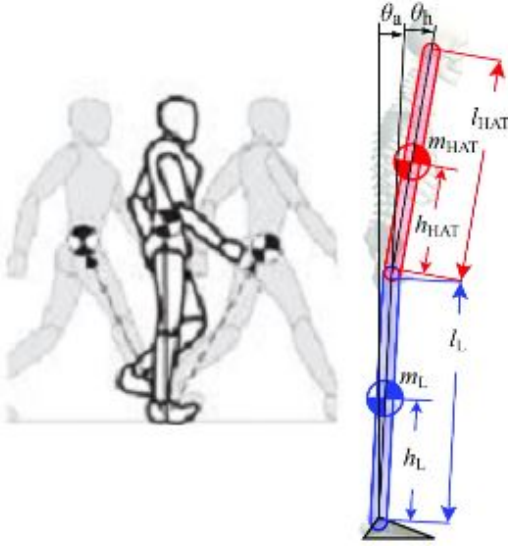


Fig. 2. (left) Inverted pendulum with COM of body as mass point, extension of double inverted pendulum case to human body (right)

While for the double inverted pendulum we keep the combined center of mass in the sagittal plane. This is what we do while we simply walk. If we divide the body in two parts we can compare it with double inverted pendulum case and while walking we subconsciously keep the center of mass in the sagittal plane so that we do not fall. Further delving into the pendulum cases we can even explore the path planning of the center of mass and then apply to human body.

#### E. Visualization

1) *3D Visualization of the motion:* For this part we use the BSP parameters calculated before. We already have the information on the specific shape and dimensions of each part of the body segment. We plot these shapes and update at every instant of time. For example, if we consider the a shape from the “Elliptical solid” group we require the five geometric parameters to construct the shape. These five values are obtained by the BSP parameters we calculated before. The function “elliptical” takes these values as an input and provides the global X,Y and Z co-ordinates. After then the update of this shape according to the respective motion and time step is taken care by the “trans\_rot” function. Sometimes, like in the case of thigh, the elliptical solid needs to be rotated about an axis so that all in all it resembles the human body. This task is done by the function “Rotation\_solid” which takes in the input as the value of the angle by which the shape is to be rotated along the specific axis. This is done for every segment of the body. For every part there are specific shapes aligned in specific direction at certain position.

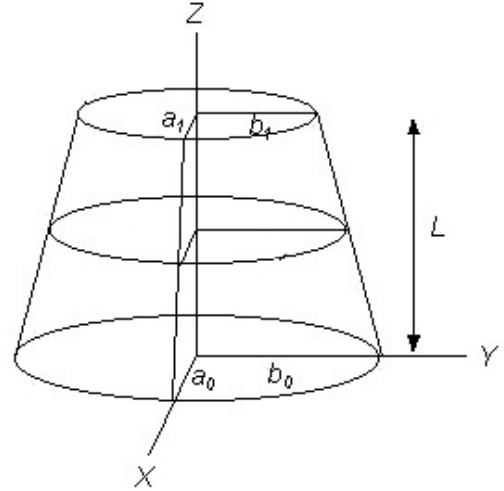


Fig. 3. Shape from the Elliptical Solid group with the 5 geometric parameters defining it

2) *Visualization of the results:* The forces and moments are plotted for the motion captured on the force plate and the one that we programmed in MATLAB. The main goal is to compare these plots but before comparing it is important to align both of these plots. For the same time period and motion we have more measurements on the force plate than the motion capture. Even if the sensor data is re-sampled to have the same frequency we have the problem of extra values of measurement on force plate. The most general reason behind this is , the recording of the force plate data started before the recording of the motion capture. Even if we try to minimize this time lag there would never be an ideal case. So, “align\_plot” function is used in this case. We have the data over an interval, by using this function we can define our own starting and ending point for the analysis. As soon as the code is run, you will be directed to select a starting point and an ending point using

the interface for the data from force plate. Similarly, after that we also chose the start and end points of the data to be read from the motion capture. We are just not considering the extra time in the beginning and the ending which gives output that is not fruitful. Using this approach we can not be perfect but we can come close to the ideal case.

#### IV. RESULTS & ANALYSIS

##### A. BSP Estimation

Measuring the 41 segments of the body for the calculation of BSP parameters is not an easy task. Moreover, each individual tends to have different way of measuring these parameters. For example, while measuring the length of the upper trunk one cannot just measure rolling the tape over the body between the markers. To get precise readings one must take the perpendicular distance between the markers, for this one must extend the markers outward by using a rigid scale or rod, keeping it steady and then measure the distance. This itself shows the task is difficult and the repeatability is not at all good. Sometimes even locating the correct marker on some body parts may be hard. Of course, this was one of the objectives of this lab to take the correct measurements by keeping the starting and the end points same for all segments for different subjects and to encounter the difficulties while measuring these values. From the data given, we observe that for all the subjects most of the measurements of the body segments lie in a similar range except for 7 (shank), 8 (thigh), 12 (Middle Trunk), 25 (Upper thigh), 26 (Head), 28 (Xiphion Level) and 41 (Neck Intersection). The measurement for Middle trunk has the highest variance and as mentioned above it is difficult to measure that part of the body. So for the analysis, we took the mean values of these measurements and calculated further.

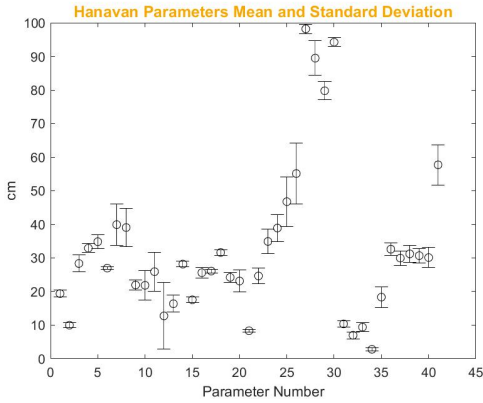


Fig. 4. Hanavan Parameters obtained.

##### B. Estimating the ground reactions

1) *Overall analysis for all the motions:* In the following subsections, the reader can find the results obtained from the MATLAB program developed. These results, as explained in the previous section, are the plots of the ground reactions measured against the ground reactions estimated for each

motion using the algorithms described. The analysis is divided in the motions performed to try to identify key points related to the effect that the velocity and acceleration have. As the reader can soon observe, there are some motions that got better results than others; however, a general analysis of the system is here presented since there are insights that apply to all motions studied. These key points are actually related to possible sources of error, that in a way represent the difficulties experimented in the current human motion study.

Regarding the modeling approach: Several strong assumptions were taken to try to get a model that behaves as the human body studied. The first point to discuss is that the BSP Parameters and the Modified Havanan Model are just an approximation, an estimation that tries to objectively describe the different parts of the human body. While, they are one of the most used models they do not guarantee reliability in the results. This is because of the way the measurements are performed, which lead to large differences between same samples, as seen in the data-set provided for the 41 parameters of the subject. The 41 parameters used in this lab, are actually the average of this data-set which could not represent truly the real dimensions of the subject. Moreover, the Modified Havanan Model categories each body part in perfect geometrical shapes which may not even fit well for all of them. Trying to model, for example, a human head as a semi ellipsoid is way too ambitious since the head is a much more complex geometrical shape. This leads to a computation of center of mass and inertia matrix far from reality.

The second point of discussion is the assumption that each body part has a constant density and that this density is equal to the average of the human body density. This assumptions, simplify the computations largely but it's far from reality. Each body part has its own density, given by the distribution of bones, muscle, water and fat. Furthermore, these values change greatly between subjects so using the average human body density is also prone to error. All this lead to a wrong estimation of the total mass of the subject and therefore a wrong estimation of the mass for each body part. Since the mass, center of mass and inertia matrix of each body part is recursively used in each computation, the error propagates to all further results. The total mass of the subject estimated, using the BSP parameters and the Modified Havanan model, is 77.66 kg against a measurement of 82.56 kg from the force plate. That is an error of almost 7 percent that will propagate along all further computations.

Regarding the algorithm: Several strong assumptions were taken to compute the ground reactions efforts applied by the subject on each motion. The first point of discussion is that the human body is not rigid. This can't be stressed enough, the human body is fundamentally flexible, the skin, the softness of the muscles and the absorption of motions by the bones definitely makes the human body far from being a theoretical rigid body. However; this is the best approach for modeling the human body, because otherwise, the algorithms and well known developed theory like the Newton Euler couldn't be applied onto the study of human motion. Moreover, under this

scope, the motion performed by the human body isn't a conservative system, which further complicates and compromise the reliability of the results obtained.

The second point of discussion is that the assumption that the efforts applied on the frame 1 are equally distributed between the two legs is actually not close to reality. This for example, doesn't hold when the subject is holding all his weight with only one leg, as the reader will observe later in the kick motions. Moreover, in this same scenario, the assumption of that the ground reaction is the sum of the efforts on both feet doesn't hold neither, adding more sources of error to the final plots shown.

Regarding the signal processing: Several strong assumptions were taken to try to get the right measurements to work with. As mentioned in the previous section, a re sample of the force plate measurement was needed in order to have both data-sets with the same frequency. This implies a process of interpolation, which corrupts the real data representing the motion performed. Further more, multiple filters were applied along the program to get better numerical values to work with. Even if this improves the behaviour of the final results because extreme peaks or highly noisy graphs are less frequent, this also worsen the raw information of the motion loss. The more the signals are filtered, the more the real information is lost. This also applies for the computation of the velocity and acceleration based on the position of the markers, the best way to deal with this was to directly measure the velocity and acceleration of each body part with dedicated sensors. Finally, since the practical experience or work with the sensors system wasn't possible, it is hard to estimate the real effects that this could have meant for the final results.

Regarding the motions: Each motion is repeated by the subject in three different speeds. However, this is essentially difficult to perform at a precise level. Motions are not exactly the same between changes of speed since it is difficult for the subject, who has little feedback about his movements, to start and end in the same joint angles as before. And from the measurement point of view, it is also difficult to check this situation on the fly. Also, it would be ideal to the subject to perform the motions as natural as possible; but, with all the markers placed and on top of the force plate sensor, the subject is far from feeling comfortable and natural.

Now that most of the possible sources of error have been discussed and analyzed, the reader can have better insights and intuition of the following graphs obtained as results of the system.

2) *Jump motions*: The jump motions are the motions that the better results were obtained. In the Fig.5, Fig.6, Fig.7, Fig.8 and Fig.9, it can be appreciated a high similarity between the ground reactions measured and estimated for the Force in the Z-axis. Sadly, this cannot be said for all other forces and moments which resulted noisy and uncorrelated.

It is fair to say that the jumps motions have the best results because when the subject's feet leave the force plate, the errors accumulated get reset. However, this is not enough to compensate the errors specifically generated by the natural

damping of the vertical impact performed instinctively by the human body, which relates to the fact of the human body not being rigid and the system not conservative.

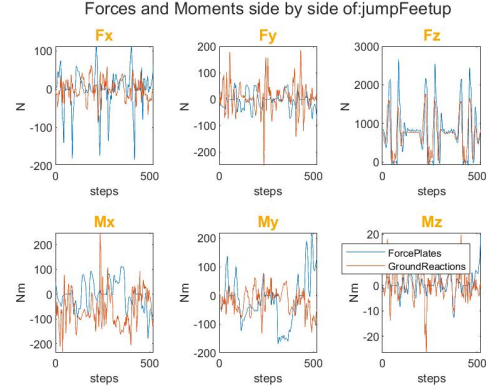


Fig. 5. Efforts obtained for motion: Jump feet up.

The Fig.5 shows a very good performance for the  $F_z$  force. The estimated graph has the same shape as the one measured and also follow the same occurrence. The difference in amplitude could be due two main reasons. The first one is that the filters applied filters the very sharp peaks, so where in the measured  $F_z$  a sharp and high peak presents, in the estimated that same peak will always be of lower amplitude. The second one is the error percentage of the mass estimated of the subject, which sets a constant offset in the graph.

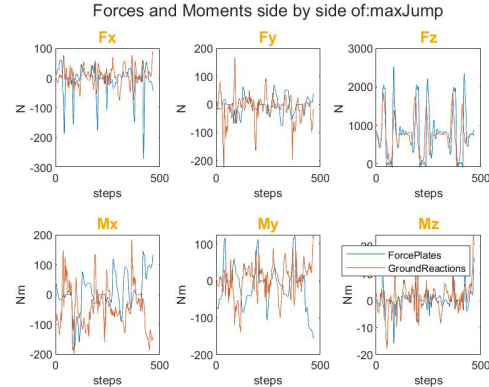


Fig. 6. Efforts obtained for motion: Max Jump.

The Fig.6, as well as the previous one, shows a good result for the  $F_z$  force estimated. However; again the other efforts don't follow the same shape as the efforts measured. The plots for the other efforts, apart from the  $F_z$ , seem to be reliable only for the magnitude order of the effort.

This same analysis apply for the rest of the jump motions results obtained. Where the  $F_z$  is a reliable estimation of its measured counterpart, being the  $M_z$  the next in line of similarity and where for the other efforts, the estimation is only truthful for the order of magnitude, since neither the shape nor the amplitude is close to their measured counterparts.



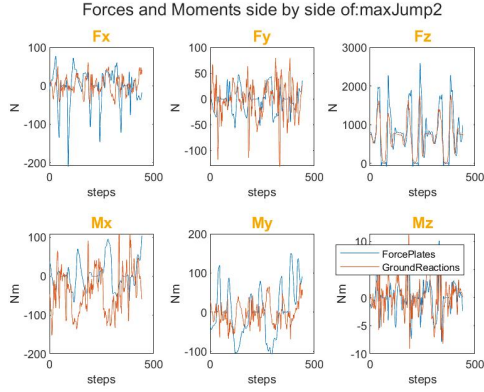


Fig. 7. Efforts obtained for motion: Max Jump2.

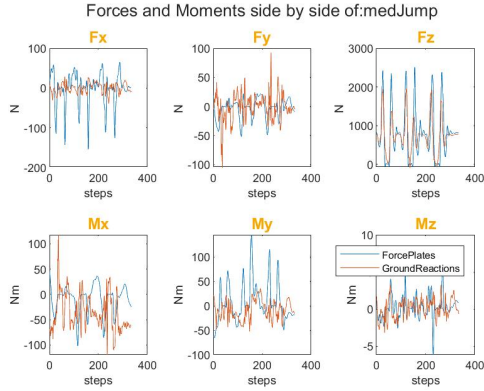


Fig. 8. Efforts obtained for motion: Med Jump.

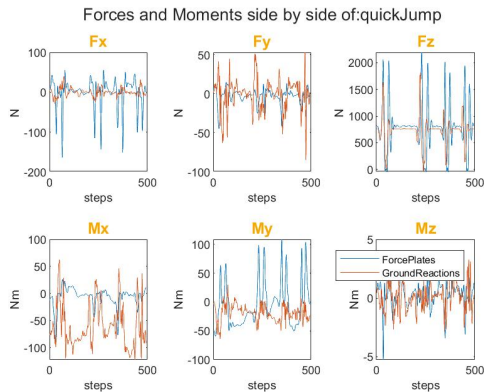


Fig. 9. Efforts obtained for motion: Quick Jump.

3) *Arm motions:* For the arm motions, we get to analyze the effect that the velocity and acceleration of the movement has on the program developed. As a first observation, again the  $F_z$  force component estimated is the one more similar to its measured counterpart. But this time this similarity is reduced to only shape, and not amplitude. It can be seen that the graphs follows the same uphill and downhill than the measured one, in a way that can be almost counted and compared one to one. However; the offset between both seems to be higher than the one for the jump motions and its amplitude looks down-scaled with respect to the measured one.

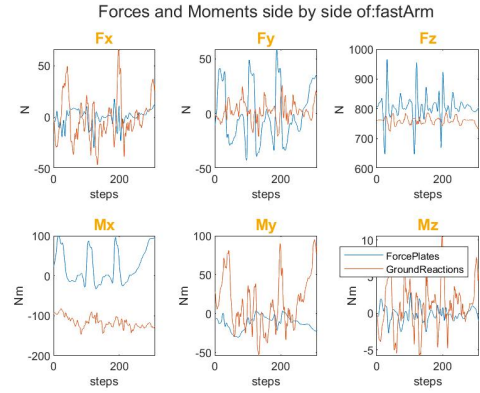


Fig. 10. Efforts obtained for motion: Fast arm.

It is interesting to note that the slow movements perform better than the rapid ones. This is expected since the velocity and acceleration for the slower movements can be better estimated following the programmatic methods used. For example, if we compare the  $F_y$  obtained for Fig.10 (fast arm) and Fig.11 (medium arm), we can notice that the medium arm graph is way better, since it looks like it follows the shape of the measured one. This confirm the thinking that slower motions gives better results.

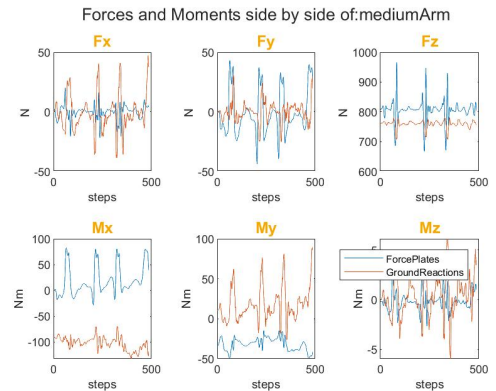


Fig. 11. Efforts obtained for motion: Medium arm.

In Fig.12 a different approach was done. All other motions, the subject always performs a stomp onto the force-plate to have an initial and easily identifiable peak in the data-set.

However, since the movement of the arm is very slightly, it is possible that the ground reactions are not recorded correctly if the force plate sensor receives an initial peak, due to the hysteresis phenomena. In the Medium arm no stomp, a more detailed graph is obtained for  $F_z$  were the periodically small peaks observed are actually the effect of the motion. This improved the estimation of all the other efforts, most of them now follow the same shape as their measured counter parts. And for the case of  $F_x$ ,  $F_y$  and  $M_z$  the amplitude also seem correctly estimated. This small but identifiable perturbations can't be observed well enough in the Fig.13, were the subject performed the stomps in between the arm waves.

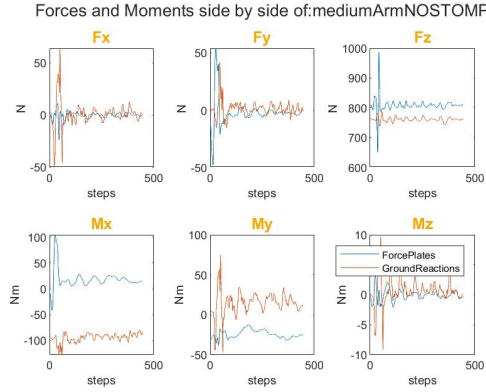


Fig. 12. Efforts obtained for motion: Medium arm no stomp.

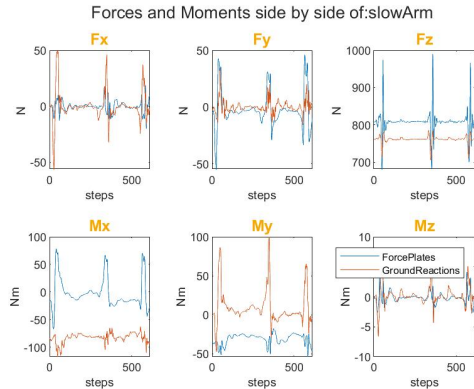


Fig. 13. Efforts obtained for motion: Slow arm.

4) *Kick motions:* Of all three types of motions performed, the kick motions are the one that present the worst results. This is because several assumptions made, explained in previous subsection, don't hold when the subject stands only on one foot. The resulted estimations are noisy and, except for  $F_z$ , don't seem to follow the shape of the measured ones. This is also due to the fact that the measured efforts themselves are highly noisy and varies their value constantly and rapidly. This of course left the system developed more prone to errors, since it is not much robust against these behaviours. As before, the results obtained are only use full to give an insight of the order

of magnitude of the efforts, since the graph can be compared much more than that, given their unstable pattern. It would also be wrong to conclude, for this set of motions, that the velocity and acceleration of the motion played a part in the estimated results, since the slow kick of Fig.16 perform similar to Fig.14.

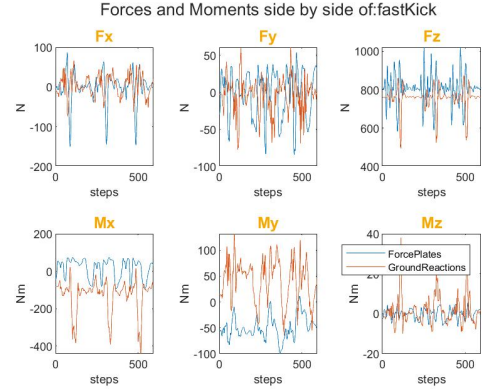


Fig. 14. Efforts obtained for motion: Fast kick.

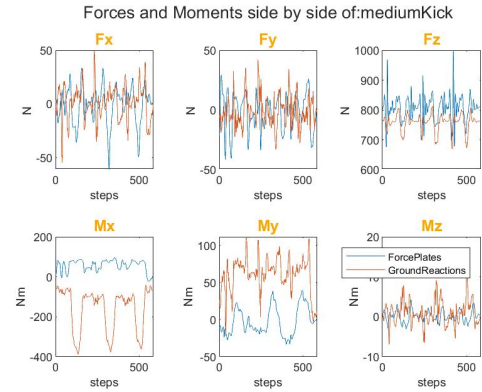


Fig. 15. Efforts obtained for motion: Medium kick.

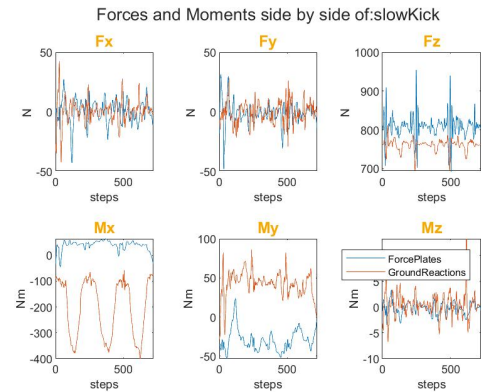


Fig. 16. Efforts obtained for motion: Slow kick.

### C. Energies

The potential and kinetic energies of all the motions were computed and plotted; however, for sake of brevity, here it is only shown one graph obtained. Since the rest are similar and the analysis applies the same for all of them. The reader can find the other energy graphs in the folder called “figures”.

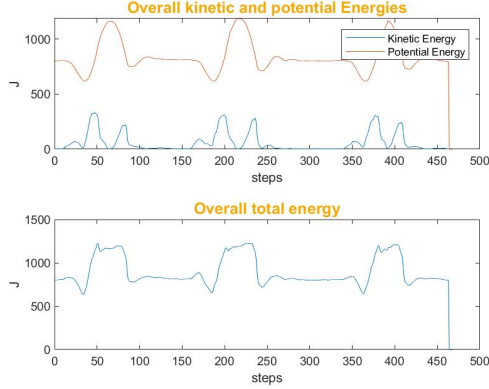


Fig. 17. Energy obtained for motion: Max Jump.

The Fig.17 shows the kinetic, potential and total energy of the whole Max jump motion. These values were computed only from the motions of each body and not from the forces and moments acting in the different body parts. However; this computation is only for sake of competition since there is no measurement of the real total energy to compare against. This doesn't mean that we can't extract valuable information out of the graphs. For example, we can see that when the jump is performed, the kinetic energy reaches its peak and once the subject is preparing for the next jump, the kinetic energy drops to zero and the total energy of the system is only composed by the potential energy caused by the weight of the subject. So the estimation of the energy follows the expected results under this scope. A further study of this data can be done by applying the work-energy theorem, relating the work produced by the forces and moments and the kinetic energy of each body part.

### D. Visualization

In the visualization part that was coded we observe that the results are satisfactory given the motion data. We can easily see and identify the different motions that were performed and recorded. We do not see a continuous smooth data because the frequency of the data recorded and the frequency at which it is shown are not in corroboration. High frequency data when recorded can also lead to noise. Moreover, as discussed earlier due to sampling of the frequency to match the force plate and motion data interpolation was done. This corrupts the data and lead some deviation in the motion performed. We also see some irregularities in the visualization. For example while jumping motion the toes of the legs go below the the ground. This is due to the fact of an assumption. We assume that the force point at the bottom of the foot where the reaction forces

are observed is below the ankle. We cannot consider the whole foot as a single point. So when the subject performs a jump, the forward part of the foot goes beyond the ground as for our consideration while computing the forces the bottom part of the ankle is reference point but it is not for the motion capture system. Given the visualization, it is more obvious that the simplified model of the human body is still far from the real one and therefore errors will always appear. But over all the results of the visualization are satisfactory.

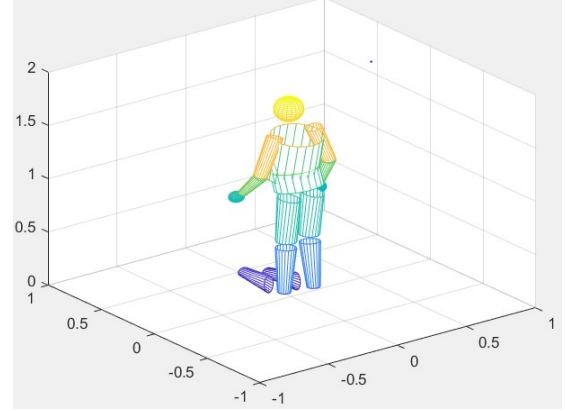


Fig. 18. Visualization of the body after integrating the positions of the parts at a time step

### V. CONCLUSIONS

- Measuring the 41 BSP parameters of a subject can be far from repetitive and reliable.
- Even making a strong assumption of the subject's body parts to have constant density, an error of 7 percent was obtained in the total mass estimate.
- Under the scope of this study, the body is undeniable non rigid and non conservative.
- The distribution of the efforts along the body assumed, affects largely the result's performance for some motions largely, specially those that at some point the subject only holds on one foot.
- Filtering the input signals and the velocity and acceleration signals estimated can be good for removing peaks and smoothing the results but important raw information of the motion is lost.
- Repeat the same motions with different speed is hard to perform for the subject and hard to identify on the fly.
- The jump motions were the ones with better results. This is especially true for the  $F_z$  effort which is reliable, repetitive and similar to its measured counterpart.
- Most of the constant offset observed in the  $F_z$  efforts in most of the motions is due to the mass estimation error.
- Slow motions tend to have better results than faster motions, at least for the arms waving motions.
- It is worth to repeat the measurements without doing the stomp every time before the motion is performed by the subject, since the measurements when it wasn't performed seem more sensible.



- The visualization developed works as expected, it serves its purpose of giving an idea of the motion done by the subject.
- Each assumption made has a significant effect on the analysis of entire system.
- Mimicking the exact human motion is a talk of future as the our primary assumption that body is rigid is preposterous.
- This analysis is not recommended for someone designing a full scale humanoid robot, several assumptions must be resolved before incorporating this method.

#### REFERENCES

- [1] Sakka, S. (2020). Lab instructions: Human Motion.
- [2] A.R.T. (2012). User Manual for ART-Human: ART-Human Version 1.0.0.
- [3] Sakka, S. (2020). From Human Motion to Humanoid Control course.